1997RMxAA..33..127R

Revista Mexicana de Astronomía y Astrofísica, **33**, 127–130 (1997)

A LONG-SLIT, HIGH RESOLUTION SPECTRUM OF THE HH 30 JET[1]

A. C. Raga[2], R. López[3], A. Riera[4], R. Estalella[3], and G. Anglada[5]

Received 1997 April 29; accepted 1997 June 15

RESUMEN

El jet HH 30 ha sido observado extensamente en el pasado. Este artículo es una adición a este cuerpo de datos, presentando un nuevo espectro de rendija larga de alta resolución (que incluye Hα y las líneas rojas de [N II] y [S II]), con una cobertura espacial de $\sim 10'$. Con este espectro, hemos determinado las velocidades radiales del jet y de su superficie de trabajo, así como las del contrajet. Encontramos que las velocidades radiales medidas parecen ser consistentes con una interpretación de HH 30 en términos de un modelo de jet curvo.

ABSTRACT

The HH 30 jet has been observed quite extensively in the past. This paper is an addition to the HH 30 data set, presenting a new long-slit, high resolution spectrum (including the Hα and red [N II] and [S II] lines), with a spatial coverage of $\sim 10'$. From this spectrum, we carry out radial velocity determinations for the jet and its working surface, as well as for the counterjet. We find that the measured velocities appear to be consistent with an interpretation of HH 30 as a curved jet.

Key words: **ISM – INDIVIDUAL OBJECTS (HH 30) — ISM – JETS AND OUTFLOWS — STARS – FORMATION**

1. INTRODUCTION

The HH 30 jet is a very interesting HH object, first noted by Mundt, Brugel, & Bührke (1987) and Mundt, Ray, & Bührke (1988). Later papers present radial velocities, proper motions, line ratios and the deconvolved width vs. position of the inner 20″ of the HH 30 jet/counterjet (Mundt et al. 1990).

The papers of López et al. (1995, 1996) discuss the spatial structure and proper motions of the HH 30 jet/counterjet in the red [S II] lines at distances of up to 5′ from the exciting source (HH 30-star). These authors detect a gradual westward curvature of the jet and counterjet, with this curvature being more pronounced for the counterjet. They also detect a collection of knots (HH 30-N) $\sim 5'$ N of the source, which they interpret as being the head of the HH 30 jet. The curvature of the jet and counterjet was previously noted by Graham & Heyer (1990) in Hα images of HH 30.

In this paper, we present a new high resolution, long-slit spectrum covering the whole region between the source and head of the HH 30 jet, as well as the region of the counterjet within 100″ of the source. From these observations (described in § 2), we obtain radial velocity measurements of most of the HH 30 jet/counterjet system (§ 3). We finally interpret these radial velocities in terms of the model of a curved jet (§ 4) suggested by López et al. (1996).

2. THE OBSERVATIONS

Spectroscopic observations were carried out on 1966 December 3-6 with the CARELEC spectrograph (Lemaître et al. 1989) attached to the Cassegrain focus of the 1.93-m telescope of the Observatoire de Haute Provence (OHP, France). The detector was a 512×512, 27 μm pixel Tektronic CCD, which provided a spatial resolution of 1.1″/pixel. The 1200 line mm^{-1} (33 Å mm^{-1}) grating was centered at λ 6557 Å, covering the spectral range from $\lambda\lambda$ 6325 Å to 6789 Å and giving a spectral resolution of 0.88 Å/pixel ($\sim$ 40 km s^{-1} resolution around Hα).

In order to obtain the spectrum of the HH30 jet

[1] Based on observations made at the Observatoire de Haute-Provence (CNRS, France).

[2] Instituto de Astronomía, Universidad Nacional Autónoma de México.

[3] Departament d'Astronomia i Meteorologia, Universitat de Barcelona, Spain.

[4] Departament de Física i Enginyeria Nuclear, Universitat Politécnica de Catalunya, Spain.

[5] Instituto de Astrofísica de Andalucía, Spain.

© Universidad Nacional Autónoma de México • Provided by the NASA Astrophysics Data System

1997RMxAA..33..127R

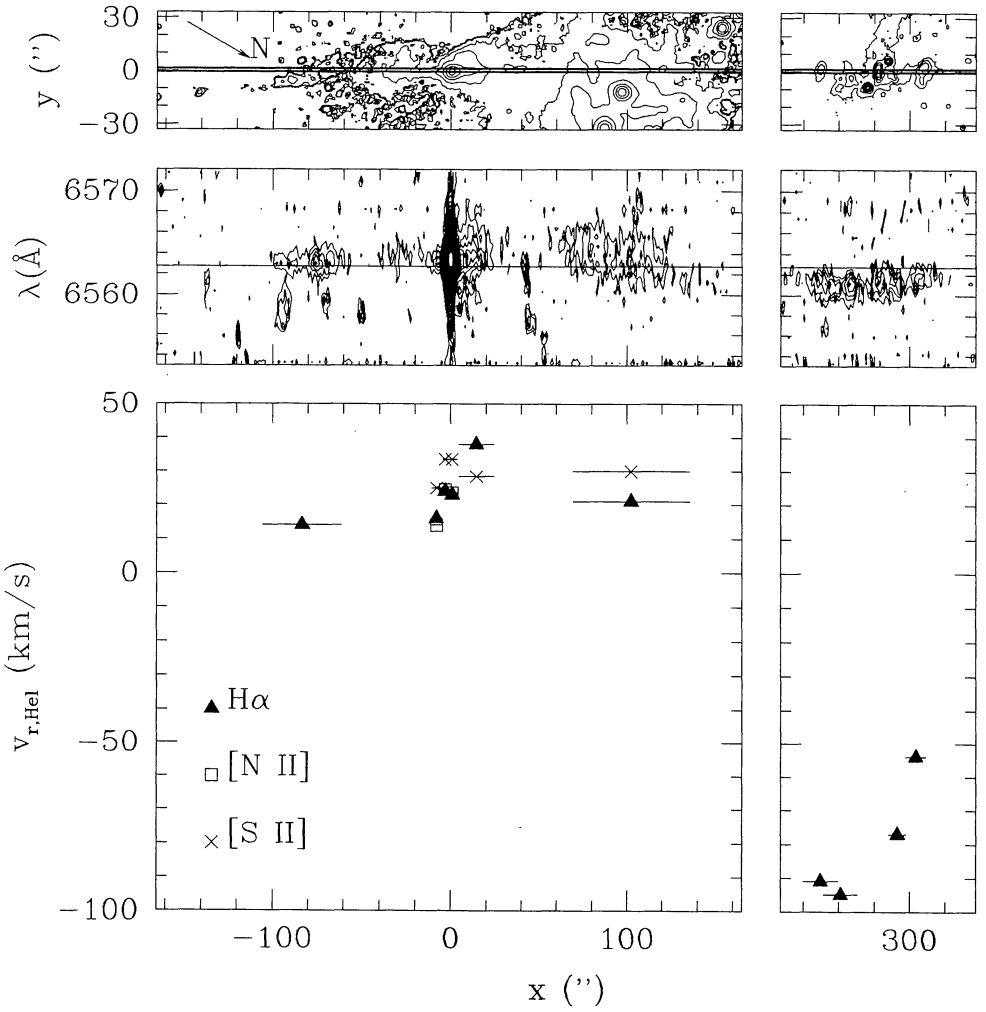

Fig. 1. [S II] 6717+31 image (top), Hα long-slit spectrum (center) and radial velocity determinations (bottom) for the HH 30 jet/counterjet system. The graphs are divided into two sections: one with the region close to the outflow source (left), and the other one with the region of the HH 30 jet working surface (right). The x-axis is aligned with an orientation of PA=30° (the direction N being indicated in the top graph), parallel with the direction of the spectrograph slits, with $(x, y) = (0, 0)$ corresponding to the approximate position of the outflow source. The slit position and width are shown on the image with the two thick, horizontal lines. The horizontal line through the position-velocity diagram indicates the laboratory wavelength of the Hα line. The bottom plot shows the heliocentric radial velocities determined for different emission lines (denoted by different symbols), for spectra that have been spatially binned over the regions indicated by the horizontal lines drawn through the points (also see Table 1).

and counterjet near the source, the slit (5'.5 long and 2 arcsec wide) was centered at the position of the HH30-star with a Position Angle (PA) of +30°. Two exposures of 1800s each were obtained. For the spectrum of HH30-N, the slit (2 arcsec wide) was centered at the position of the NE knot given in López et al. (1996), at a PA of +30°. Four exposures of 1800s each were then obtained in order to get a total integration time of 2 hours. Calibration exposures were frequently obtained along the night.

All the spectra were processed for bias and flat-field corrections, using the standard IRAF tasks. The extraction of the spectra included a background substraction to remove the sky emission. The wavelength scale was set by a fit to a Cu-Ar calibration lamp. The wavelength calibration obtained was better than 0.1 Å . Weather conditions were not photometric, thus the spectra were not flux-calibrated.

3. THE RADIAL VELOCITIES OF THE HH 30 JET

From the two long-slit spectra that we have obtained, it is possible to measure the radial velocity structure of the northern jet (knots B-I), the southern counterjet (knots F-N), and the northern working surface (knots NA-NH of López et al. 1995). In order

© Universidad Nacional Autónoma de México • Provided by the NASA Astrophysics Data System

1997RMxAA..33..127R

to improve the signal-to-noise ratio we have first spatially binned the spectrum, and we have then carried out Gaussian fits to determine the radial velocity for each bin.

The results of this process are shown in Figure 1. In this figure, we show a [S II] image of HH 30 with the position of the spectrograph slit, the Hα position-velocity diagram, and the radial velocities measured for Hα and the red [N II] and [S II] lines. These radial velocities are also given in Table 1.

If we average all of the radial velocity determinations for the region within 20″ of the source, we obtain a velocity $< v_s >= 26$ km s^{-1}. Averaging the radial velocities obtained for the $30 < x < 125''$ region (see Fig. 1), we obtain an average velocity $< v_j >= 26$ km s^{-1} for the jet. With the velocities in the $-100'' < x < -60''$ region, we obtain a velocity $< v_c >= 14$ km s^{-1} for the counterjet. Finally, for the working surface ($240'' < x < 310''$, see Fig. 1) we obtain an average radial velocity $< v_{ws} >= -79$ km $^{-1}$s.

Using these average radial velocities, we can determine average values for the velocity gradients. For the jet ($0 < x < 125''$), we obtain $\nabla_j \equiv < dv/dx >_j \approx 0$. For the counterjet ($-100'' < x < 0$), we obtain $\nabla_c \approx 0.15$ km s^{-1} arcsec^{-1}. Finally, for the region from the source out to the northern working surface, we obtain $\nabla_{ws} \approx -0.38$ km s^{-1} arcsec^{-1}.

From this, we see that the radial velocity gradient along the jet is initially ~ 0, and then grows quite substantially approaching the region of the northern working surface. Along the counterjet, the velocity gradient is much larger than the one of the jet at $\sim 1'$ from the source. At larger distances from the source we do not see the counterjet, since it falls outside the spectrograph slit due to its quite pronounced curvature in the plane of the sky (see Fig. 1 and López et al. 1995).

It is interesting to note that if one looks at Fig. 1, it appears that in the $0 < x < 60''$ region, the radial velocity of the jet might grow quite appreciably, and then decrease again towards zero radial velocity in the $60'' < x < 130''$ region. This effect, however, is hard to quantify due to the low signal-to-noise ratio of this region of our long-slit spectrum. Deeper spectra will be necessary for carrying out a quantitative study of this structure.

We should note that the Hα line profile near the source (i.e., $x \approx 0$ in Fig. 1) is likely to be contaminated by the emission line profile of the central star itself. *Hubble Space Telescope (HST)* observations of the region around the source of HH 30 show the presence of a strong reflection nebula (Stapelfeldt et al. 1997), which is also to some extent visible in previous Hα images. This stellar contribution would of course affect our radial velocity measurements for the region close to the outflow source. However, the fact that the radial velocities at the position of the source (see Table 1) agree quite well for all of the measured lines probably indicates that the effect of the stellar contribution does not modify the measured velocities in a dramatic way.

4. DISCUSSION

The radial velocity structure of the HH 30 jet/counterjet shows a quite unique behaviour. The heliocentric velocity close to the source has a value $< v_s >= 25.7$ km s^{-1}. This velocity lies quite close

TABLE 1

HELIOCENTRIC RADIAL VELOCITIES

				v_{Hel}[d]				
	Knot[a]	d[b] (″)	Size[c] (″)	[N II]$_{6548}$ (km s^{-1})	Hα (km s^{-1})	[N II]$_{6584}$ (km s^{-1})	[S II]$_{6717}$ (km s^{-1})	[S II]$_{6731}$ (km s^{-1})
HH 30 jet	J-K	−80.3	31.9	...	+14	...	...	...
	F	−8.3	8.8	...	+16	+14	+25	+25
	HH 30	0.0	6.6	+21	+24	+28	+36	+31
	A	+5.0	4.4	+20	+23	+27	...	...
	B-D	+12.7	11.0	...	+38	...	+25	+32
	G-I	+97.9	49.5	...	+21	...	+30	...
HH 30 N	NA	+249.6	19.8	...	−91	...	...	...
	NC	+265.5	9.9	...	−95	...	...	...
	NF-NG	+293.0	9.9	...	−77	...	...	...
	NH	+303.5	11.0	...	−54	...	...	...

[a]From López et al. (1995). [b]Distance of the center of the region from the HH 30-star position. [c]Size of the regions over which the spectra have been binned. [d]The errors in the heliocentric radial velocities are ~ 12 km s^{-1}, except for knots B-D for which the uncertainties are ~ 20 km s^{-1}.

© Universidad Nacional Autónoma de México • Provided by the NASA Astrophysics Data System

1997RMxAA..33..127R

to the velocity $v_{Hel} = 19$ km s^{-1} of the surrounding cloud (see Mundt et al. 1990; Snell, Loren, & Plambeck 1980).

As one moves away from the source, the radial velocity decreases in the directions of both the jet and the counterjet, becoming negative in the region of the northern head of the HH 30 jet. This behaviour can be interpreted in terms of a jet and counterjet which are ejected close to the plane of the sky, and then curve towards the observer at larger distances from the source. This of course qualitatively agrees with the fact that the HH 30 jet/counterjet system shows a quite remarkable curvature (with both jet and counterjet curving westward) in the plane of the sky (see López et al. 1995). The proper motion measurements of the northern head of the HH 30 jet of López et al. (1996), also show evidence of a curvature of the flow in the plane of the sky.

It is also notable that the fact that the counterjet has a more highly curved morphology than the jet (in the images of López et al. 1995) is apparently reflected in the radial velocities. The HH 30 jet has an average radial velocity $< v_j >= 25.5$ km s^{-1}, which is not significantly different from the velocity $< v_s >= 25.7$ km s^{-1} of the region close to the source. On the other hand, the counterjet has an average velocity $< v_c >= 14$ km s^{-1}, which is significantly lower. The higher velocity gradient observed on the side of the counterjet is qualitatively consistent with the fact that the counterjet is more strongly curved than the jet (in the plane of the sky).

The radial velocities of highest moduli are observed for the northern head of the HH 30 jet (HH 30-N), which has an average velocity $< v_{ws} >= -79$ km s^{-1}. Unfortunately, we do not have radial velocity measurements of the counterjet at distances of $\sim 5'$ from the source to compare with the radial velocity of the northern head.

To conclude, we find that the radial velocities measured for the HH 30 jet/counterjet system appear to be consistent with the model of a curved jet which was suggested by López et al. (1995, 1996; based on the morphology and proper motion measurements). However, we find that it is still not possible to carry out a quantitative comparison between the observations of HH 30 and models of curved HH jets ejected from a source in motion with respect to the surrounding environment (Cantó & Raga 1995). For such a comparison to be significant, it will be necessary to obtain high resolution spectra with signal-to-noise ratios higher than the present spectrum, as well as obtaining better proper motion measurements than the ones of López et al. (1996). Since the HH 30 knots are quite faint and diffuse, this will require an observational program extending over several years.

Finally, we would like to point out that it is still not completely clear whether or not the HH 30-N knots are indeed associated with the HH 30 jet. There are other jet-like objects in the region, and HH 30-N could actually be associated with one of them. For example, the HL Tauri jet (Mundt et al. 1988) could give rise to the HH 30-N knots, as it points approximately in their direction (López et al. 1995). However, we judge that the present evidence appears to point to an association of HH 30-N with the HH 30 jet.

ARa acknowledges support from CONACYT and DGAPA (UNAM). GA, RE, RL and ARi acknowledge support from Spanish DGICYT PB95-0066. We thank an anonymous referee for very helpful comments.

REFERENCES

Cantó, J., & Raga, A. C. 1995, MNRAS, 277, 1120
Graham, J. A., & Heyer, M. H. 1990, PASP, 102, 972
Lemaître, G., Kohler, D., Lacroix, D., Meunier, J.-P., & Vin, A., 1989, A&A, 228, 546
López, R., Raga, A. C., Riera, A., Anglada, G., & Estalella, R. 1995, MNRAS, 274, L19
López, R., Riera, A., Raga, A. C., Anglada, G., López, J. A., Noriega-Crespo, A., & Estalella, R. 1996, MNRAS, 282, 470
Mundt, R., Brugel, E. W., & Bührke, T., 1987, ApJ, 319, 275
Mundt, R., Ray, T. P., & Bührke, T., 1988, ApJ, 333, L69
Mundt, R., Ray, T. P., Bührke, T., Raga, A. C., & Solf, J. 1990, A&A, 232, 37
Snell, R. L., Loren, R. B., & Plambeck, R. L. 1980, ApJ, 239, L37
Stapplefeldt, K. R. and the WFPC2 Science Team, 1997, in IAU Colloquium 163, Accretion Phenomena and Related Outflows, (Dordrecht: Reidel), in press

G. Anglada: Instituto de Astrofísica de Andalucía, CSIC, Ap. 3004, C/ Sancho Panza S/N, E-18080 Granada, Spain (guillem@iaa.es).
R. Estalella and R. López: Departament d'Astronomia i Meteorologia, Universitat de Barcelona, Av. Diagonal 647, E-08028 Barcelona, Spain (rosario@mizar.am.ub.es, robert@mizar.am.ub.es).
A. C. Raga: Instituto de Astronomía, UNAM, Apartado Postal 70-264, 04510 México, D.F., México (raga@astroscu.unam.mx).
A. Riera: Departament de Física i Enginyeria Nuclear, Universitat Politécnica de Catalunya, Av. Víctor Balaguer s/n, E-0800 Barcelona, Spain (angels@pro.eupvg.upc.es).

© Universidad Nacional Autónoma de México • Provided by the NASA Astrophysics Data System